

Chemical Science

rsc.li/chemical-science



ISSN 2041-6539



ROYAL SOCIETY
OF CHEMISTRY

Celebrating
IYPT 2019

EDGE ARTICLE

Kazushi Mashima *et al.*

Dinuclear manganese alkoxide complexes as catalysts for C–N bond cleavage of simple tertiary *N,N*-dialkylamides to give esters

Cite this: *Chem. Sci.*, 2019, 10, 2860

All publication charges for this article have been paid for by the Royal Society of Chemistry

Dinuclear manganese alkoxide complexes as catalysts for C–N bond cleavage of simple tertiary *N,N*-dialkylamides to give esters†

Haruki Nagae,[†] Takahiro Hirai,[†] Daiki Kato,[†] Shusei Soma,[†] Shin-ya Akebi[†] and Kazushi Mashima^{†*}

Amide bonds are stable due to the resonance between the nitrogen lone pair and the carbonyl moiety, and therefore the chemical transformation of amides, especially tertiary amides, involving C–N bond fission is considered one of the most difficult organic reactions, unavoidably requiring harsh reaction conditions and strong acids or bases. We report the catalytic C–N bond cleavage of simple tertiary *N,N*-dialkylamides to give corresponding esters using a catalyst system (2 mol% based on Mn atoms) of a tetranuclear manganese alkoxide, [Mn(acac)(OEt)(EtOH)]₄ (**1c**), combined with four equivalents of 4,7-bis(dimethylamino)-1,10-phenanthroline (**L1**: Me₂N-Phen). Regarding the reaction mechanism, we isolated a dinuclear manganese complex, [Mn(acac)(OEt)(Phen)]₂ (**6c**), which was revealed as the catalytically active species for the esterification of tertiary amides.

Received 31st December 2018
Accepted 28th January 2019

DOI: 10.1039/c8sc05819a

rsc.li/chemical-science

Introduction

Amides are ubiquitous and abundant in a huge number of natural and synthetic organic compounds, such as proteins, poly(amides), and pharmaceuticals, due to the extraordinarily stable nature of the amide bond.^{1–5} The stability of the amide bond is attributed to the resonance between the nitrogen lone pair and the carbonyl moiety, and many researchers have attempted to diminish the resonance structure of the C–N bond by introducing the coordination of transition metals to the nitrogen atom, as exemplified by the complexation of *N,N*-(2-pyridylmethyl)amides with Cu(II) sources,^{6,7} and constructing a twisted structure around the nitrogen atom,^{8,9} whose amide bonds were readily cleaved under mild conditions. Nonetheless, cleavage of the amide bond requires harsh reaction conditions such as using stoichiometric amounts of strong acids or bases at a high temperature. TiCl₄- and FeCl₃-catalyzed alcoholysis of inactivated primary amides was independently reported by Fisher *et al.* and Sun *et al.* but more than one equivalent of aqueous HCl was necessary.¹⁰ Shimizu *et al.* reported catalytic esterification of primary amides without using any additives by utilizing CeO₂ as a heterogeneous catalyst under a high reaction temperature.¹¹ Thus, catalytic transformation of amides to the corresponding esters or acids in an atom- and step-economical manner is in high demand. Recently, we reported a catalytic

C–N bond cleavage of primary and secondary amides using a catalyst mixture of Sc(OTf)₃ and boronic esters,¹² and Atkinson *et al.* also reported Sc(OTf)₃-catalyzed esterification of secondary amides.¹³ In addition, catalytic esterification of 8-aminoquinoline amides was achieved with Ni(tmhd)₂ (TMHD = 2,2,6,6-tetramethyl-3,5-heptanedionate) in methanol.¹⁴

In contrast, the catalytic transformation of tertiary amides remains a challenging task, and only a few catalyst systems developed to date are able to break the stable C–N bond of tertiary amides. Recently, Garg and Houk reported that nickel(0) complexes served as catalysts to activate the C–N bond of tertiary amides bearing functional groups such as Ph or Boc *via* oxidative addition as a key step to afford the corresponding esters (Fig. 1A),^{15–17} and Danoun and Gosmini reported that low-valent cobalt species supported by 2,2'-bipyridine using metallic manganese as a reductant catalytically activated the C–N bond of activated amides bearing a Boc group to give the corresponding esters (Fig. 1B),¹⁸ though the oxidative addition of the C–N bond of activated amides bearing functional groups such as Ph, Boc, and Ts on the nitrogen atom into low-valent transition metals was reported to be involved in several catalytic reactions.^{17,19–26} On the other hand, we reported a catalytic C–N bond cleavage of *N*-alkyl-*N*-β-hydroxyethylamides *via* *N,O*-acyl rearrangement by manganese complexes supported by an *N*[^]*N*-bidentate ligand²⁷ and zinc complexes (Fig. 1C),²⁸ though these catalysts required substrates with functional groups, such as a β-hydroxyethyl group on the nitrogen atom. Very recently, Shimizu and Siddiki reported the first example of the esterification of *N,N*-dialkylamides using CeO₂ as a reusable heterogeneous catalyst, though the catalyst system requires a high reaction temperature and large amount of catalyst. In this

Department of Chemistry, Graduate School of Engineering Science, Osaka University, Toyonaka, Osaka 560-8531, Japan. E-mail: mashima@chem.es.osaka-u.ac.jp

† Electronic supplementary information (ESI) available. CCDC 1865079, 1865080. For ESI and crystallographic data in CIF or other electronic format see DOI: 10.1039/c8sc05819a



Fig. 1 Catalytic esterification via the C–N bond cleavage of tertiary amides.

reaction, Lewis acid and base sites of the CeO₂ surface cooperatively activate the carbonyl moiety and alcohol (Fig. 1D).²⁹ To achieve the esterification of simple *N,N*-dialkyl tertiary amides under milder reaction conditions, we focused our attention on cooperative activation of multinuclear complexes whose multi-metallic structure is often found in metalloenzymes. Herein, we report a new and efficient catalyst system of [Mn(acac)(OEt)(EtOH)]₄ (**1c**), as Mn(II) precursors to evaluate the general tendency that metal-alkoxide species accelerate the nucleophilic attack of the alkoxide group on the carbonyl group (2 mol% based on Mn atom), and 4,7-bis(dimethylamino)-1,10-phenanthroline (**L1**: Me₂N-Phen) (2 mol%) for the esterification of simple tertiary *N,N*-dialkylamides to give the corresponding esters with broad substrate scopes including halogenated amides (Fig. 1E). Furthermore, we determined a reaction mechanism by isolating an alkoxide-bridged manganese dinuclear complex [Mn(acac)(OEt)(Phen)]₂ (**6c**) as the key catalyst, and measuring kinetic studies in *n*-butanol which showed first-order rate dependence on the concentrations of *N,N*-dimethyl-2-naphthamide (**2a**) and **6c**, indicating that the dinuclear alkoxide complex acted as a catalytically active species.

Results and discussion

We began by searching for the suitable catalyst among the reported alkoxy-bridged tetranuclear complexes, [M(tmhd)(OMe)(MeOH)]_x (**1**; M = Mn,^{30a} Fe,^{30b} Co,³¹ and Cu;³² 1.0 mol%; $x = 1$ or 0; TMHD = 2,2,6,6-tetramethyl-3,5-

heptanedionate), as catalyst precursors with 4,7-bis(dimethylamino)-1,10-phenanthroline (**L1**: Me₂N-Phen, 1 mol%) for the catalytic esterification of *N,N*-dimethyl-2-naphthamide (**2a**) under the conditions of using *n*-butanol (0.25 mL) at reflux temperature for 18 h, and the results are shown in Table 1.³³ The use of the manganese tetranuclear complex, [Mn(tmhd)(OMe)(MeOH)] (**1a**), afforded **3a** in 80% yield (entry 1). Iron and cobalt tetranuclear complexes exhibited lower catalytic activities (16% and 42% yields, respectively, entries 2 and 3) than the manganese complex. The copper tetranuclear complex, [Cu(tmhd)(OMe)]₄, which does not have methanol as a ligand, also showed low catalytic activity (49% yield, entry 4). Accordingly, we selected the manganese complex as the best catalyst precursor among the tetranuclear complexes, [M(tmhd)(OMe)(MeOH)]_x, we tested.

Next, we searched for the best manganese precursor for the catalytic esterification of **2a** with *n*-butanol under the conditions of Mn precursors (1 mol% based on Mn atoms) and **L1** (1 mol%) at reflux temperature for 18 h, and the results are shown in Table 2. The manganese tetranuclear alkoxide complex [Mn(dbm)(OMe)(MeOH)]₄ (**1b**: DBM = dibenzoylmethanate)^{30a} exhibited almost the same catalytic activity as **1a** to give the corresponding ester **3a** in 79% yield (entry 1), and a newly synthesized manganese complex, [Mn(acac)(OEt)(EtOH)]₄ (**1c**), showed the highest catalytic activity among the alkoxy-bridged tetranuclear complexes to yield **3a** in 90% yield (entry 2). We also surveyed other simple Mn precursors such as Mn(acac)₂, Mn(tmhd)₂, Mn(hfac)₂ (HFAC = hexafluoroacetylacetonate), and Mn(OAc)₂ but these catalyst precursors showed moderate activity to afford **3a** in 85%, 57%, 52%, and 57% yields, respectively (entries 3–6). In the absence of the **L1** ligand, **1c**

Table 1 Screening of alkoxy-bridged tetranuclear complexes

$2\text{-naph} \begin{array}{c} \text{O} \\ \parallel \\ \text{C} \\ \\ \text{N}(\text{Me})_2 \end{array} \xrightarrow[\text{cat. (1 mol\% on metal)}]{\text{L1 (Me}_2\text{N-phen, 1 mol\%)}} \begin{array}{c} \text{O} \\ \parallel \\ \text{C} \\ \\ \text{O}^i\text{Bu} \end{array}$ <p><i>n</i>BuOH (0.25 mL), 135 °C, 18 h – HNMe₂</p> <p>2a (0.5 mmol) 3a</p>		
Entry	cat.	Yield [%] ^a
1	[Mn(tmhd)(OMe)(MeOH)] ₄ (1a)	80
2	[Fe(tmhd)(OMe)(MeOH)] ₄	16
3	[Co(tmhd)(OMe)(MeOH)] ₄	42
4	[Cu(tmhd)(OMe)] ₄	49

M = Mn, Fe, and Co

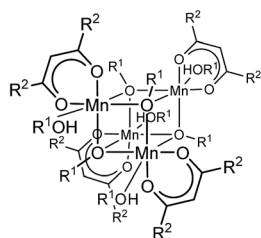
M = Cu

^a Determined by GC analysis with dodecane as an internal standard.



Table 2 Screening of manganese precursors

$\text{2-naph-NMe}_2 \xrightarrow[\text{- HNMe}_2]{\text{[Mn] (X mol\% on Mn), Me}_2\text{N-Phen (L1: X mol\%)}, n\text{BuOH (0.25 mL), 135 }^\circ\text{C, 18 h}}$ $\text{2-naph-O}^n\text{Bu}$			
Entry	[Mn]	X [mol%]	3a: Yield ^a [%]
1	1b	1	79
2	1c	1	90
3	Mn(acac) ₂	1	85
4	Mn(tmhd) ₂	1	57
5	Mn(hfac) ₂	1	52
6	Mn(OAc) ₂	1	57
7 ^b	1c	1	22
8	1c	2	>99
9 ^c	-	1	n.r. ^e
10 ^d	-	1	n.r. ^e



1a: R¹ = Me, R² = ^tBu
1b: R¹ = Me, R² = Ph
1c: R¹ = Et, R² = Me

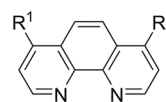
^a Determined by GC analysis with dodecane as an internal standard.
^b Without **L1**. ^c 1 mol% of KOMe was used as the catalyst instead of **1c**. ^d 1 mol% of NaOMe was used as the catalyst instead of **1c**. ^e n.r. = No reaction.

exhibited low catalytic activity (entry 7, 22% yield). The yield of **3a** was increased to >99% when increasing the catalyst loading of **1c** to 2 mol% (entry 8). The use of 1 mol% of strong bases, such as KOMe and NaOMe, did not result in catalytic activity (entries 9 and 10). Thus, we selected catalyst **1c** as the best precursor, and optimized the conditions using 2 mol% of **1c** and **L1** in *n*-butanol at reflux temperature for 18 h. Under the optimized reaction conditions, we detected signals of cationic manganese dinuclear complexes, [Mn(acac)(OⁿBu)(Me₂N-Phen)]₂⁺ (*m/z* = 986.4) and [Mn(acac)(OⁿBu)(Me₂N-Phen)]₂ + H⁺ (*m/z* = 987.4), by ESI-MS spectroscopy. In addition, we isolated a dinuclear complex, [Mn(acac)(OEt)(Phen)]₂, and characterized it by single crystal X-ray analysis (*vide infra*).

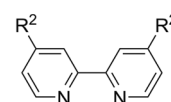
We then searched for a suitable chelating nitrogen ligand for the catalytic esterification of *N,N*-dimethyl-2-naphthamide (**2a**) under the conditions of using [Mn(acac)(OEt)(EtOH)]₄ (**1c**: 1.0 mol%) and a nitrogen ligand (1.0 mol%) in refluxing *n*-butanol (5.5 equiv.) for 18 h, and the results are shown in Table 3. We first used 1,10-phenanthroline derivatives **L2**–**L7**. Electron-donating groups at 4,7-positions on 1,10-phenanthroline exhibited remarkable substituent effects for increasing catalytic activities: **L2** with methoxy groups, **L3** with methyl groups, and **L5** with phenyl groups produced **3a** in moderate

Table 3 Screening of ligands

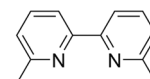
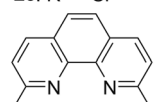
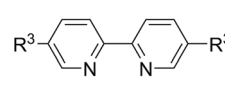
$\text{2-naph-NMe}_2 \xrightarrow[\text{- HNMe}_2]{\text{[Mn(acac)(OEt)(EtOH)]}_4 \text{ (1c) (1 mol\% on Mn), Ligand (Y mol\%)}, n\text{BuOH (0.25 mL), 135 }^\circ\text{C, 18 h}}$ $\text{2-naph-O}^n\text{Bu}$			
Entry	Ligand	Y	Yield [%] ^a
1	L2	1	67
2	L3	1	54
3	L4	1	36
4	L5	1	68
5	L6	1	27
6	L7	1	49
7	L8	1	23
8	L9	1	20
9	L10	1	31
10	L11	1	33



L1: R¹ = NMe₂
L2: R¹ = OMe
L3: R¹ = Me
L4: R¹ = H
L5: R¹ = Ph
L6: R¹ = Cl



L8: R² = OMe
L9: R² = ^tBu
L10: R² = Me
L11: R² = H
L12: R² = COOMe

**L15****L7**

L13: R³ = Me
L14: R³ = CF₃



L16: R⁴ = H
L17: R⁴ = 4-Me
L18: R⁴ = 4-NMe₂
L19: R⁴ = 4-CN
L20: R⁴ = 2,6-Me₂

^a Determined by GC analysis with dodecane as an internal standard.

yields (67%, 54%, and 68%, respectively; entries 1, 2, and 4). In contrast, 1,10-phenanthroline (**L4**) and **L6** with electron-withdrawing chloro groups exhibited decreased catalytic activity, affording 36% and 27% yields of **3a**, respectively (entries 3 and 5). The sterically congested chelating nitrogen ligand 2,9-dimethyl-1,10-phenanthroline (**L7**) gave **3a** in 49% yield (entry 6). 4,4'-Substituted 2,2'-bipyridine derivatives, such as **L8** with methoxy groups, **L9** with *tert*-butyl groups, **L10** with methyl groups, 2,2'-bipyridine (**L11**), and **L12** with methyl ester groups, exhibited low catalytic activities (entries 7–11). In addition, 5,5'-dimethyl-2,2'-bipyridine (**L13**), 5,5'-bis(trifluoromethyl)-2,2'-bipyridine (**L14**), and 6,6'-dimethyl-2,2'-bipyridine (**L15**) produced **3a** in low yields (28%, 19%, and 14%, respectively, entries 12–14). Monodentate pyridine derivatives **L16**–**L20** afforded **3a** in 16%, 18%, 19%, 29%, and 20% yields, respectively (entries 15–19), which was almost the same as the catalytic activity of **1c** without any ligand (Table 2, entry 7).



Consequently, we selected **L1** as the best ligand for $[\text{Mn}(\text{acac})(\text{OEt})(\text{EtOH})]_4$ (**1c**) with 2 mol% catalyst loading.

We next evaluated the substrate scope for the esterification of *N,N*-dimethylamides (Table 4). *N,N*-dimethylbenzamide (**2b**) afforded *n*-butyl benzoate (**3b**) in a good yield (78%, entry 1). The electronic effects of the *para*-position on *N,N*-dimethylbenzamide were examined: **2c** having a methoxy group slightly decreased the yield to 65% (entry 2), while substrates **2d** and **2e** with a trifluoromethyl group at the *para*- and *meta*-positions afforded **3d** and **3e** in the same high yield as **3b** (**3d**: 84%, **3e**: 77% yields, entries 3 and 4). Benzamides **2f–h** having chloro, bromo, and iodo atoms at the *para*-position gave the corresponding products **3f–h** in high yield without any loss of the C–X bond (entries 5–7). Notably, in the case of methyl substituted compounds, the steric congestion around the carbonyl moiety of the amides was crucial: 4-methyl- and 3-methyl derivatives **2i** and **2j** produced **3i** in 77% yield and **3j** in 27% yield, while *N,N*-dimethyl-2-methylbenzamide (**2k**) led to a trace amount of **3k** (entries 8–10). 4-Cyano-*N,N*-dimethylbenzamide (**2l**) gave **3l** in 86% yield (entry 11). On the other hand, the use of an aliphatic substituted amide, *N,N*-dimethyl-3-phenylpropanamide, afforded 12% of the corresponding ester **3m** (entry 12). *N,N*-Dimethylisonicotinamide (**2n**) and *N,N*-dimethyl-2-furamide (**2o**) were converted to the corresponding esters **3n** and **3o** in 98% and 88% yields, respectively (entries 13 and 14).

We varied the alcohols used for the esterification of **2a** (Table 5). We used alcohols with a low boiling point and

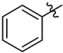
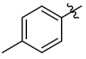
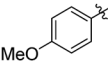
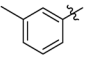
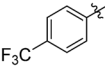
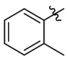
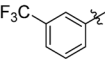
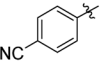
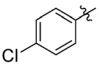
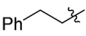
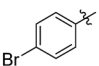
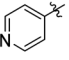
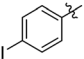
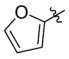
Table 5 Scope and limitation of alcohols

$\text{2-naph-C(=O)NMe}_2 \xrightarrow[\text{- HNMe}_2]{\text{1c (4 mol\% on Mn), L1 (4 mol\%)}} \text{2-naph-C(=O)OR}$			
Entry	R	Temp. [°C]	4: Yield ^a [%]
1		120 °C	4a : 93
2 ^b			4a : 78
3 ^c		140 °C	4b : 69
4 ^c		135 °C	4c : 43
5		170 °C	4d : 78
6 ^{d,e}		135 °C	4e : 51
7 ^d		135 °C	4f : 92
8 ^d		135 °C	4g : 61
9 ^{c,d}		135 °C	4h : 53

^a Isolated yield. ^b 2 mol% of **1c** (based on Mn) and **L1** were used.

^c Reaction time was 72 h. ^d 1.2 equiv. of alcohol was used in toluene solution. ^e Reaction time was 18 h.

Table 4 Scope and limitation of amides 2

<div><div><div><div><div><div></div><div>R^1</div></div><div><div><div><div><div><div></div><div>$\text{C}=\text{O}$</div><div>NMe_2</div></div></div><div>$\xrightarrow[\text{- HNMe}_2]{\text{1c (2 mol\% on Mn), L1 (2 mol\%)}}$</div><div><div><div><div><div><div></div><div>R^1</div></div><div><div><div><div><div><div></div><div>$\text{C}=\text{O}$</div><div>O^nBu</div></div></div></div></div></div><div>3</div></div></div><div>$^n\text{BuOH (0.25 mL), 135 }^\circ\text{C, 18 h}$</div></div></div></div></div></div></div></div></div></div>					
Entry	R ¹	3: Yield ^a [%]	Entry	R ¹	3: Yield ^a [%]
1 ^b		2b 3b : 78	8 ^b		2i 3i : 77
2 ^b		2c 3c : 65	9		2j 3j : 27
3		2d 3d : 84	10		2k 3k : trace ^c
4		2e 3e : 77	11		2l 3l : 86
5		2f 3f : 92	12		2m 3m : 12
6		2g 3g : 78	13		2n 3n : 98
7		2h 3h : 86	14		2o 3o : 88

^a Isolated yield. ^b Reaction time was 45 h. ^c Determined by ¹H NMR analysis with phenanthrene as an internal standard.

sterically bulky secondary alcohols, and modified the reaction conditions by increasing the loading of **1c** to 4 mol% based on Mn metal with **L1** (4 mol%) and using a longer reaction time depending on the alcohols we assessed. The reaction with *n*-propanol at reflux temperature (120 °C) for 45 h gave *n*-propyl benzoate (**4a**) in 93% yield, although the reaction of *n*-propanol with 2 mol% of **1c** and **L1** for 45 h afforded **4a** in lower yields (78%) (entries 1 and 2). Secondary alcohols such as 2-pentanol and 3-pentanol, respectively, afforded **4b** and **4c** in 69% and 43% yields at reflux temperature (140 °C and 135 °C, respectively) for 72 h (entries 3 and 4), while 4-heptanol produced the corresponding ester **4d** in 78% yield at reflux temperature (170 °C) for 72 h (entry 5). Solid alcohols such as 2,2-dimethylpropanol, (4-methylphenyl)methanol, and piperonyl alcohol could be used for the esterification of **2a** in toluene at 135 °C, giving the corresponding esters **4e** (51% yield for 18 h reaction time), **4f** (92% yield), and **4g** (61% yield) (entries 6–8). When 3-methyl-1,3-butanediol was used for the esterification, 3-hydroxy-3-methylbutyl-2-naphthoate (**4h**) was selectively obtained in a moderate yield (53% yield, entry 8).

In contrast to the catalytic esterification of *N,N*-dimethylamides, in which volatile dimethylamine was readily removed, the addition of 1 equiv. of diethyl carbonate was required to trap liberated amines to accomplish smooth esterification of various substituents on the nitrogen atom of benzamide under conditions of using **1c** (5 mol% based on Mn atom) with **L1**



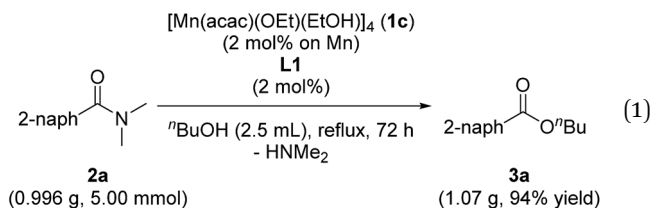
Table 6 Substrate scope for benzamides 5

$ \begin{array}{c} \text{Ph}-\text{C}(=\text{O})-\text{N}(\text{R}^2)-\text{R}^3 \\ \text{5 (0.5 mmol)} \end{array} \xrightarrow[\text{diethyl carbonate (1.0 equiv)}]{\text{1c (5 mol\% on Mn), L1 (5 mol\%)}} \begin{array}{c} \text{Ph}-\text{C}(=\text{O})-\text{O}^n\text{Bu} \\ \text{3b} \end{array} $			$ \begin{array}{c} \text{Ph}-\text{C}(=\text{O})-\text{N}(\text{R}^2)-\text{R}^3 \\ \text{5 (0.5 mmol)} \end{array} \xrightarrow[\text{diethyl carbonate (1.0 equiv)}]{\text{1c (5 mol\% on Mn), L1 (5 mol\%)}} \begin{array}{c} \text{Ph}-\text{C}(=\text{O})-\text{O}^n\text{Bu} \\ \text{3b} \end{array} $		
Entry	5	3b: Yield ^a (%)	Entry	5	3b: Yield ^a (%)
1		81(74)	6		92
2		88	7		60
3		76	8		83
4		25	9		82
5		93			

^a Determined by GC analysis with dodecane as an internal standard. Isolated yield is given in parentheses.

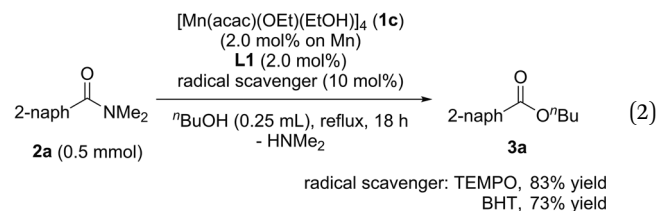
(5 mol%) in refluxing *n*-butanol for 45 h (Table 6). Cyclic derivatives of benzamide with piperidine **5a**, morpholine **5b**, and pyrrolidine **5c** were converted into *n*-butyl benzoate **3b** in 81%, 88%, and 76% yields, respectively (entries 1–3), though acyclic *N,N*-diethylbenzamide (**5d**) significantly decreased the yield of **3b**, (25%, entry 4), probably due to the steric hindrance around the carbonyl group of **5d**. Esterification of *N*-methyl-*N*-phenylbenzamide (**5e**) and 1-benzoyl pyrrole (**5f**) gave **3b** in 93% and 92% yields, respectively (entries 5 and 6). Moreover, the manganese catalyst system effectively mediated the esterification of secondary and primary amides, such as *N*-methylbenzamide (**5g**: 60% yield), *N*-(quinolin-8-yl)benzamide (**5h**: 83% yield), and benzamide (**5i**: 82% yield) (entries 7–9).

When we conducted a large scale reaction by using 0.996 g of **2a** under the conditions of using **1c** (2.0 mol%) and **L1** (2.0 mol%) in refluxing *n*-butanol (2.5 mL, 5.5 equiv.) for 72 h, we obtained 1.07 g of corresponding **3a** in 94% yield (eqn (1)).



When radical scavengers, such as TEMPO and BHT, were added to the reaction mixture, the yields of **3a** were slightly decreased to 83% and 73%, respectively, and by-products containing TEMPO or BHT moieties were not detected (eqn (2)).

Thus, we proposed that the reaction mechanism is not a radical pathway.



Regarding the reaction mechanism, we isolated an alkoxide-bridged Mn(II) dinuclear complex, [Mn(acac)(OEt)(Phen)]₂ (**6c**: 47% yield), by treating complex **1c** with 1,10-phenanthroline (**L4**) (eqn (3)), as the corresponding manganese complex containing Me₂N-Phen (**L1**) provided no single crystals suitable for X-ray analysis. Complex **6c** was characterized by elemental analysis and X-ray analysis due to its paramagnetic nature. In the solid state, complex **6c** has a dimeric structure, in which two manganese centers are doubly bridged by two μ -ethoxy groups and each manganese atom adopts a distorted octahedral structure (Fig. 2).



Fig. 2 Molecular structures of complex **1c** and **6c** with 50% thermal ellipsoids. All hydrogen atoms and solvent molecule are omitted for clarity.

We determined a power value on the concentration of substrate **2a** using time normalization analysis.^{34a} A mixture of **2a** (0.600, 0.800, and 1.00 M) and [Mn(acac)(OEt)(Phen)]₂ (**6c**, 60.7 mg, 80 μ mol, 40 mM) in *n*-butanol (2.00 mL) with dodecane as an internal standard was refluxed at 145 $^\circ$ C and the time course of the yield of **3a** was determined by GC analysis. As shown in Fig. 3, the concentration of **3a** was plotted against a normalized time scale, $\sum [2a]^a \Delta t$, and we adjusted the power value, *a*, until all the corrected conversion curves overlay. As a result, we determined that the value of *a* was 1 (Fig. 3c). We



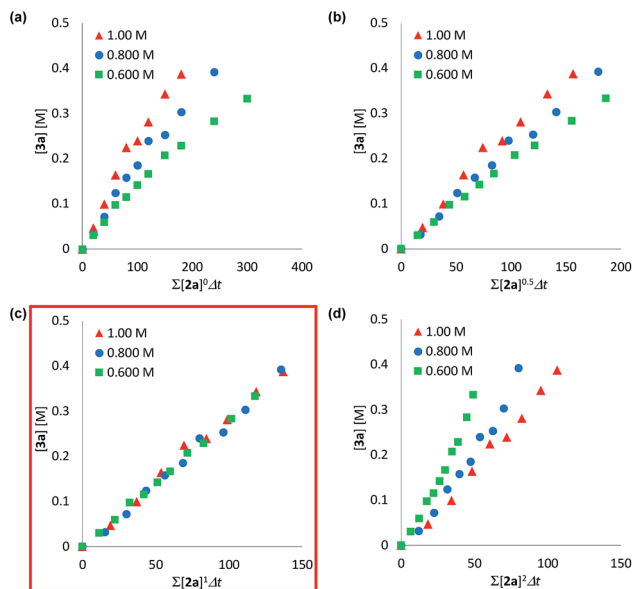


Fig. 3 Time normalization analysis to determine the order in amide **2a**; (a) $a = 0$, (b) $a = 0.5$, (c) $a = 1$, (d) $a = 2$.

also determined a power value on the concentration of the catalyst $[\text{Mn}(\text{acac})(\text{OEt})(\text{Phen})]_2$ (**6c**) by using a normalized time scale analysis.^{34b} A mixture of **2a** (398.5 mg, 2.00 mmol, 2.00 M) and **6c** (30 mM, 50 mM, and 70 mM) in *n*-butanol (1.00 mL) with dodecane as an internal standard was refluxed at 145 °C. As shown in Fig. 4, the concentration of **3a** was plotted against a normalized time scale, $t[\text{6c}]^n$, and we determined that the value of n was 1 (Fig. 4c). The first-order rate dependency of **6c** suggested that the dinuclear manganese complex **6c** acted as a catalytically active species, whose dinuclear function was comparable to that found for an alkoxide-bridged cobalt dinuclear complex active for catalytic transesterification.³⁵

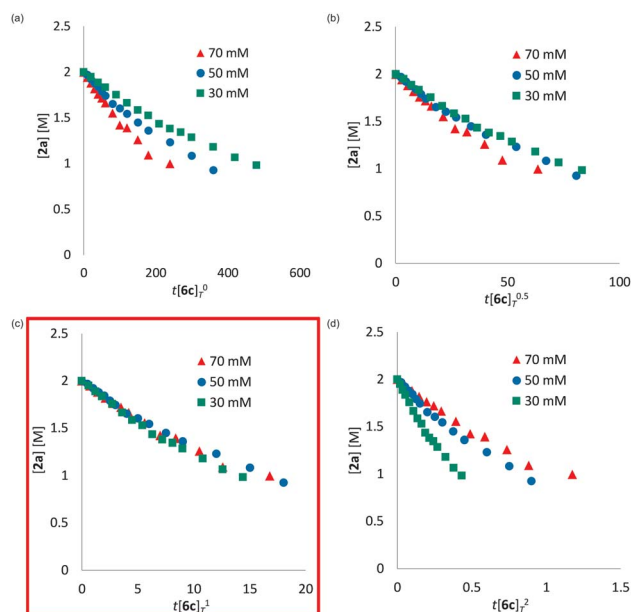
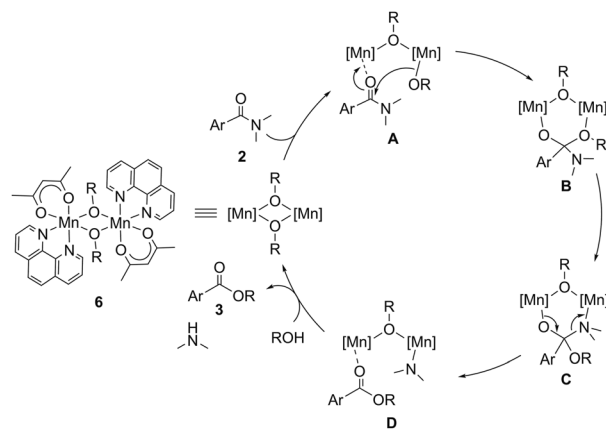


Fig. 4 Time normalization analysis to determine the order in dinuclear manganese complex **6c**; (a) $a = 0$, (b) $a = 0.5$, (c) $a = 1$, (d) $a = 2$.



Scheme 1 A plausible reaction mechanism for the catalytic esterification of simple tertiary *N,N*-dimethylamides.

On the basis of these results, we propose a reaction mechanism of the catalytic esterification of simple tertiary *N,N*-dimethylamides described in Scheme 1. The first step is the coordination of amide **2** onto a manganese atom of complex **6c**, affording dinuclear complex **A**. The alkoxy group bound to the manganese center in **A** attacks the carbonyl group of the amide moiety to cleave a C–N bond *via* intermediate **B**, in which an *N,N*-bidentate ligand with electron-donating groups at the *para*-positions accelerated the nucleophilic attack. According to the kinetics, the nucleophilic attack of the alkoxide on the carbonyl group is the rate-determining step. The intermediate **B** is transformed to **C**, forming a manganese complex **D**, where the resulting ester coordinates to the manganese atom bearing a dimethylamido moiety. Finally, protonolysis of the manganese-amido moiety using alcohol produces dimethylamine and the dinuclear Mn(II)-alkoxide complex together with the release of ester **3**.

Conclusions

In summary, we provide the first example of catalytic esterification of simple tertiary *N,N*-dialkylamides under neutral conditions using the catalyst system $[\text{Mn}(\text{acac})(\text{OEt})(\text{EtOH})]_4$ (**1c**, 2 mol% based on Mn metal) and 4,7-bis(dimethylamino)-1,10-phenanthroline (**L1**: Me₂N-Phen, 2 mol%). Regarding the reaction mechanism, we isolated the alkoxide-bridged manganese dinuclear complex $[\text{Mn}(\text{acac})(\text{OEt})(\text{Phen})]_2$ (**6c**) as the key catalyst, and conducted kinetic studies in which the velocity obeys $k_{\text{obs}}[\text{2a}]^1[\text{6c}]^1$. It is notable that such a catalytic performance of the dinuclear manganese complex **6c** is related to the mechanism of metalloenzymes that regulate the transformation of carboxylic derivatives. Further mechanistic studies and catalytic application of a Mn-based catalyst system are ongoing in our laboratory.

Experimental section

All manipulations involving air- and moisture-sensitive organometallic compounds were carried out under argon using the



standard Schlenk technique or an argon-filled glovebox. *n*-Propanol, 2-propanol, *n*-butanol, 2-pentanol, 3-pentanol, 4-heptanol, and diethyl carbonate were distilled under an argon atmosphere from CaH₂. 3-Methyl-1,3-butanediol was distilled under an argon atmosphere by using Kugelrohr. 2,4-Pentadione was distilled under an argon atmosphere from P₄O₁₀. THF, diethyl ether, hexane, and toluene were dried and deoxygenated using a Grubbs column (Glass Contour Solvent Dispensing System, Nikko Hansen & Co., Ltd.).³⁶ Ethanol and methanol were distilled under an argon atmosphere from the corresponding magnesium alkoxide. DMSO-*d*₆ was dried over MS4A in a J-Young Schlenk under an argon atmosphere. Wako super dehydrated DMF was degassed and kept in a J-Young Schlenk with MS4A under an argon atmosphere. Lithium ethoxide was prepared by treating metal lithium with ethanol in hexane suspension. All other reagents were purchased from commercial resources and used without further purification. NMR spectra were recorded on a Bruker AV 400M spectrometer operating at 400 MHz (¹H NMR), at 100 MHz (¹³C{¹H} NMR) and at 376 MHz (¹⁹F{¹H} NMR) in 5 mm NMR tubes. All ¹H NMR chemical shifts were reported in ppm relative to the TMS at 0.00 ppm or residual solvent protons in DMSO-*d*₆ at δ 2.50. All ¹³C{¹H} NMR chemical shifts were reported in ppm relative to carbon resonance in chloroform-*d*₁ at δ 77.16 and DMSO-*d*₆ at δ 39.52. All ¹⁹F{¹H} NMR chemical shifts were reported in ppm relative to the external reference α,α,α -trifluorotoluene at δ -63.9. Melting points were recorded using a BUCHI Melting Point M-565 and YANACO MP-J3. IR spectra were recorded on a JASCO FT/IR 4000 spectrometer. Mass spectra (MS) and high resolution mass spectra (HRMS) were recorded using a JEOL JMS-700. ESI-mass spectrometric data were obtained using a BRUKER microTOF-II spectrometer. GC analyses were recorded on a Shimadzu GC-2014 gas chromatograph with J&W Scientific DB-5 and Shimadzu SH-Rtx-50 columns. Flash column chromatography was performed using silica gel 60 (0.040–0.063 mm, 230–400 mesh ASTM).

General procedure for catalytic esterification of *N,N*-dimethyl-2-naphthamide (1.0 mol%)

The mixture of catalyst precursor (5.0 μ mol based on Mn atoms), ligand (5.0 μ mol), and *N,N*-dimethyl-2-naphthamide (99.6 mg, 5.00 $\times 10^{-1}$ mmol) in *n*-butanol (2.50 $\times 10^{-1}$ mL) was refluxed at 135 °C for 18 hours under an argon atmosphere in a slim Schlenk (ϕ 10 mm). After cooling to room temperature, yields were determined using the following procedures.

(1) GC yield: metal salts were removed by filtration through silica gel with ethyl acetate. The yield was determined by GC analysis with dodecane as an internal standard.

(2) NMR yield: metal complexes were removed by filtration through silica gel with CDCl₃ twice. The yield was determined by ¹H NMR analysis with phenanthrene as an internal standard.

General procedure for preparation of amides

Amides were synthesized by standard condensation reaction using the corresponding acyl chlorides and amines. Products were purified by silica gel flash column chromatography or

distillation under reduced pressure using Kugelrohr, and characterized by ¹H and ¹³C{¹H} NMR spectroscopies.

Preparation of ligands, substrate amides, and manganese complexes

Synthesis of 1-benzoyl pyrrole (5f). Equivalents of substrates were modified from the literature.³⁷ Sodium hydride (60% oil dispersion, 599.8 mg, 15.0 mmol) was washed with 2 mL of dried and deoxygenated hexane three times under an argon atmosphere, and dried *in vacuo*. After refilling argon, dried and deoxygenated THF (20 mL) was added, and the suspension was cooled to 0 °C in an ice bath. Pyrrole (0.690 mL, 10.0 mmol) was slowly added to the reaction mixture and the mixture was stirred at 0 °C for 90 minutes. Then benzoyl chloride (1.70 mL, 15.0 mmol) was slowly added to the mixture at 0 °C. After warming to room temperature, the reaction mixture was stirred overnight. Then, the reaction mixture was quenched by water, and the water layer was extracted with 20 mL of EtOAc three times. The combined organic layer was washed with 1 M HCl aq. twice, sat. NaHCO₃ aq., and brine, and dried over Na₂SO₄. The crude products were obtained by removal of solvent *in vacuo*, and purified by flash column chromatography (silica gel, hexane : EtOAc = 20 : 1), and distillation using Kugelrohr (>0.05 mmHg, 125–135 °C) to give a colorless liquid (1.23 g, 7.18 mmol, 72% yield).

Synthesis of 4,7-bisdimethylamino-1,10-phenanthroline (Me₂N-Phen).³⁸ A suspension of 4,7-dichloro-1,10-phenanthroline (1.48 g, 5.94 mmol) in DMF (50 mL) was refluxed for 30 h under an argon atmosphere. After cooling to room temperature, all volatiles were removed *in vacuo*. Then the residue was dissolved in 1 M NaOH aq. (50 mL) and THF (70 mL), and the solution was extracted with DCM (50 mL \times 3). The combined organic layer was washed with 1 M NaOH aq. twice and brine, and dried over Na₂SO₄. Removal of volatiles *in vacuo* gave the crude product as a brown solid, and the product was purified by washing with EtOAc (3 mL \times 3) to give a purple solid (741.1 mg, 2.78 mmol, 47% yield). ¹H NMR (400 MHz, DMSO-*d*₆, 30 °C) δ 8.74 (d, *J* = 5.0 Hz, 2H), 7.96 (s, 2H), 7.11 (d, *J* = 5.0 Hz, 2H), 3.01 (s, 12H); ¹³C{¹H} NMR (100 MHz, DMSO-*d*₆, 30 °C) δ 157.0, 149.4, 147.6, 121.4, 120.6, 109.6, 43.7.

Synthesis of [Mn(tmhd)(OMe)(MeOH)]₄ (1a). [Mn(tmhd)(OMe)(MeOH)]₄ was prepared according to the literature.^{30a} MnCl₂ (629 mg, 5.00 mmol) and 2,2,6,6-tetramethylheptanedione (1.00 mL, 5.00 mmol, 1.0 equiv.) were dissolved in 10 mL of methanol. In another flask, KOMe (701 mg, 10 mmol, 2.0 equiv.) was dissolved in methanol. The two solutions were slowly mixed to form a yellow precipitate. The supernatant was removed by using a cannula, and the residues were extracted with toluene, and layered with methanol to induce recrystallization to give **1a** as a yellow solid in 82% yield (1.23 g, 1.02 mmol).

Synthesis of [M(n)(tmhd)(OMe)(MeOH)]₄ (M = Fe,^{30b}Co,³¹Cu³²). [M(n)(tmhd)(OMe)(MeOH)]₄ was prepared according to the literature. MCl₂ and 2,2,6,6-tetramethylheptanedione (1.0 equiv.) were dissolved in methanol. In another flask, KOMe (2.0 equiv.) was dissolved in methanol. The two solutions were



slowly mixed to form a precipitate, immediately. The supernatant was removed by using a cannula, and the residues were extracted with toluene, and layered with methanol to induce recrystallization. M = Fe: deep red solid, 1.09 g, 0.900 mmol, 80% yield, M = Co: burgundy solid, 152 mg, 0.124 mmol, 64% yield, M = Cu: deep blue solid, 22.2 mg, 20.0 μ mol, 11% yield.

Synthesis of [Mn(dbm)(OMe)(MeOH)]₄ (1b).^{30a} MnCl₂ (629 mg, 5.00 mmol) and dibenzoylmethane (1.12 g, 5.00 mmol, 1.0 equiv.) were dissolved in 10 mL of methanol. In another flask, KOMe (10 mmol, 2.0 equiv.) was dissolved in methanol. The two solutions were slowly mixed, and yellow powder was immediately precipitated. The supernatant was removed by using a cannula, and the residues were extracted with toluene, and layered with methanol to induce recrystallization to give **1b** as an orange solid (258 mg, 0.189 mmol, 15% yield).

Synthesis of [Mn(acac)(OEt)(EtOH)]₄ (1c). MnCl₂ (629 mg, 5.00 mmol) and acetylacetone (0.530 mL, 5.00 mmol, 1.0 equiv.) were dissolved in 10 mL of ethanol. In another flask, LiOEt (10 mmol, 2.0 equiv.) was dissolved in ethanol. The two solutions were slowly mixed, and yellow powder was immediately precipitated. The supernatant was removed by using a cannula, and the residues were extracted with toluene, and layered with ethanol to induce recrystallization to give **1c** as a pale yellow solid (1.00 g, 1.02 mmol, 82% yield). m.p. 282–290 °C (dec.), anal. calcd for C₃₆H₇₂O₁₆Mn₄: C, 44.09; H, 7.40; found: C, 43.96; H, 7.69.

Synthesis of Mn(II) alkoxide-bridged binuclear complex 6c. A solution of **1c** (99.6 mg, 0.101 mmol) and 1,10-phenanthroline (73.2 mg, 0.406 mmol, 4.00 equiv.) in toluene (10 mL) was heated at 100 °C for 18 hours under an argon atmosphere. Then, the residues were extracted with toluene (20 mL) at 100 °C, and the solution was slowly cooled to –20 °C. The supernatant was removed by using a cannula, and the resulting solid was dried under reduced pressure to give a deep red solid (71.3 mg, 0.0940 mmol, 47% yield). m.p. 230–234 °C (dec.), anal. calcd for C₃₈H₄₀N₄O₆Mn₂: C, 60.16; H, 5.31; N, 7.39; found: C, 60.10; H, 5.27; N, 7.14.

X-ray crystallographic analyses. Crystals of **1c** and **6c** were handled similarly. The crystal was mounted on a CryoLoop (Hampton Research Corp.) with a layer of light mineral oil and placed in a nitrogen stream at 113(1) K. Measurements were made on a Rigaku XtaLAB P200 system with graphite-monochromated Mo-K α (0.71075 Å) radiation. The structures of complexes **1c** and **6c** were solved using direct methods (SIR92)³⁹ in the CrystalClear program.⁴⁰ The structures were refined on F² using the full-matrix least-squares method, using SHELXL-2013.⁴¹ H-atoms were included in the refinement on calculated positions riding on their carrier atoms. The function minimized was $\sum w(F_o^2 - F_c^2)^2$ ($w = 1/[\sigma^2(F_o^2) + (aP)^2 + bP]$), where $P = (\max(F_o^2, 0) + 2F_c^2)/3$ with $\sigma^2(F_o^2)$ from counting statistics. The functions R1 and wR2 were $(\sum ||F_o| - |F_c||)/\sum |F_o|$ and $[\sum w(F_o^2 - F_c^2)^2/\sum (wF_o^4)]^{1/2}$, respectively. Crystal data and structure refinement parameters are listed in Table S1.† The ORTEP-3 program was used to draw the molecules.⁴²

Conflicts of interest

There are no conflicts to declare.

Acknowledgements

This work was supported by JSPS KAKENHI Grant Numbers JP26248028 and JP16H06934, Grant-in-Aid for Scientific Research(A) and Grant-in-Aid for Young Scientists (Start-up). We thank Ms Shoko Akiyama for her experimental contribution in the early stage of the project.

Note and references

- 1 A. Greenberg, C. M. Berneman and J. F. Liebman, *The Amide Linkage: Structural Significance in Chemistry and Biotechnology and Materials Science*, John Wiley & Sons, Ltd., 2003.
- 2 H. Lundberg, F. Tinnis, N. Selander and H. Adolfsson, *Chem. Soc. Rev.*, 2014, **43**, 2714–2742.
- 3 J. M. García, F. C. García, F. Serna and J. L. de la Peña, *Prog. Polym. Sci.*, 2010, **35**, 623–686.
- 4 R. Das, G. S. Kumar and M. Kapur, *Eur. J. Org. Chem.*, 2017, 5439–5459.
- 5 S. A. Glover and A. A. Rosser, *J. Org. Chem.*, 2012, **77**, 5492–5502.
- 6 R. P. Houghton and R. R. Puttner, *J. Chem. Soc. D*, 1970, 1270–1271.
- 7 M. C. Bröhmer, S. Munding, S. Bräse and W. Bannwarth, *Angew. Chem., Int. Ed.*, 2011, **50**, 6175–6177.
- 8 A. J. Kirby, I. V. Komarov, P. D. Wothers and N. Feeder, *Angew. Chem., Int. Ed.*, 1998, **37**, 785–786.
- 9 M. Szostak and J. Aubé, *Chem. Rev.*, 2013, **113**, 5701–5765.
- 10 (a) L. E. Fisher, J. M. Caroon, S. R. Stabler, S. Lundberg, S. Zaidi, C. M. Sorensen, M. L. Sparacino and J. M. Muchowski, *Can. J. Chem.*, 1994, **72**, 142–145; (b) X. Chen, S. Hu, R. Chen, J. Wang, M. Wu, H. Guo and S. Sun, *RSC Adv.*, 2018, **8**, 4571–4576.
- 11 S. M. A. H. Siddiki, A. S. Touchy, M. Tamura and K. Shimizu, *RSC Adv.*, 2014, **4**, 35803–35807.
- 12 Y. Kita, Y. Nishii, A. Onoue and K. Mashima, *Adv. Synth. Catal.*, 2013, **355**, 3391–3395.
- 13 B. N. Atkinson and J. M. J. Williams, *Tetrahedron Lett.*, 2014, **55**, 6935–6938.
- 14 T. Deguchi, H.-L. Xin, H. Morimoto and T. Ohshima, *ACS Catal.*, 2017, **7**, 3157–3161.
- 15 L. Hie, N. F. Fine Nathel, T. K. Shah, E. L. Baker, X. Hong, Y.-F. Yang, P. Liu, K. N. Houk and N. K. Garg, *Nature*, 2015, **524**, 79–83.
- 16 L. Hie, E. L. Baker, S. M. Anthony, J.-N. Desrosiers, C. Senanayake and N. K. Garg, *Angew. Chem., Int. Ed.*, 2016, **55**, 15129–15132.
- 17 J. E. Dander and N. K. Garg, *ACS Catal.*, 2017, **7**, 1413–1423.
- 18 Y. Bourne-Branchu, C. Gosmini and G. Danoun, *Chem.-Eur. J.*, 2017, **23**, 10043–10047.
- 19 X. Li and G. Zou, *Chem. Commun.*, 2015, **51**, 5089–5092.
- 20 G. Meng and M. Szostak, *Org. Lett.*, 2015, **17**, 4364–4367.
- 21 C. Liu and M. Szostak, *Chem.-Eur. J.*, 2017, **23**, 7157–7173.



- 22 J. Hu, M. Wang, X. Pu and Z. Shi, *Nat. Commun.*, 2017, **8**, 14993.
- 23 S.-C. Lee, L. Guo, H. Yue, H.-H. Liao and M. Rueping, *Synlett*, 2017, **28**, 2594–2598.
- 24 A. Dey, S. Sasmal, K. Seth, G. K. Lahiri and D. Maiti, *ACS Catal.*, 2017, **7**, 433–437.
- 25 J. A. Walker Jr, K. L. Vickerman, J. N. Humke and L. M. Stanley, *J. Am. Chem. Soc.*, 2017, **139**, 10228–10231.
- 26 C. W. Cheung, J.-A. Ma and X. Hu, *J. Am. Chem. Soc.*, 2018, **140**, 6789–6792.
- 27 Y. Nishii, S. Akiyama, Y. Kita and K. Mashima, *Synlett*, 2015, **26**, 1831–1834.
- 28 Y. Nishii, T. Hirai, S. Fernandez, P. Knochel and K. Mashima, *Eur. J. Org. Chem.*, 2017, 5010–5014.
- 29 T. Toyano, M. N. Rashed, Y. Morita, T. Kamichi, S. M. A. H. Siddiki, M. A. Ali, A. S. Touchy, K. Kon, Z. Maeno, K. Yoshizawa and K. Shimizu, *ChemCatChem*, 2019, **11**, 449–456.
- 30 (a) L. E. Pence, A. Caneschi and S. J. Lippard, *Inorg. Chem.*, 1996, **35**, 3069–3072; (b) K. L. Taft, A. Caneschi, L. E. Pence, C. D. Delfs, G. C. Papaefthymiou and S. J. Lippard, *J. Am. Chem. Soc.*, 1993, **115**, 11753–11766.
- 31 J. F. Berry, F. A. Cotton, C. Y. Liu, T. Lu, C. A. Murillo, B. S. Tsukerblat, D. Villagrán and X. Wang, *J. Am. Chem. Soc.*, 2005, **127**, 4895–4902.
- 32 W. H. Watson and W. W. Holley, *Croat. Chem. Acta*, 1984, **57**, 467–476.
- 33 *N,N*-Dimethylamide could not be used as a substrate in Ni(0) catalysed esterification (see ref. 15). In addition, the esterification of **2a** by the catalyst system Mn(acac)₂ (10 mol%) with 2,2'-bipyridine (10 mol%), which is the same as our previous catalyst system (see ref. 27), in *n*BuOH at reflux temperature for 18 h afforded the corresponding ester **3a** in 68% yield.
- 34 (a) J. Burés, *Angew. Chem., Int. Ed.*, 2016, **55**, 2028–2031; (b) J. Burés, *Angew. Chem., Int. Ed.*, 2016, **55**, 16084–16087.
- 35 Y. Hayashi, S. Santoro, Y. Azuma, F. Himo, T. Ohshima and K. Mashima, *J. Am. Chem. Soc.*, 2013, **135**, 6192–6199.
- 36 A. B. Pangborn, M. A. Giardello, R. H. Grubbs, R. K. Rosen and F. J. Timmers, *Organometallics*, 1996, **15**, 1518–1520.
- 37 C. K. Lee, J. H. Jun and J. S. Yu, *J. Heterocycl. Chem.*, 2000, **37**, 15–24.
- 38 P. Wehman, V. E. Kaasjager, F. Hartl, P. C. J. Kamer, P. W. N. M. van Leeuwen, J. Fraanje and K. Goubitz, *Organometallics*, 1995, **14**, 3751–3761.
- 39 A. Altomare, G. Casciarano, C. Giacovazzo and A. Guagliardi, *J. Appl. Crystallogr.*, 1993, **26**, 343–350.
- 40 *CrystalClear: Data Collection and Processing Software*, Rigaku Corporation, 1998–2015, Tokyo 196-8666, Japan.
- 41 G. M. Sheldrick, *Acta Crystallogr., Sect. A: Found. Crystallogr.*, 2008, **64**, 112–122.
- 42 L. J. Farrugia, *J. Appl. Crystallogr.*, 1997, **30**, 565.

